Bulk Polymerization of Styrene in the Presence of Polybutadiene: Effect of Initiator Type and Prepolymerization Conditions on Particle Morphology

G. Soto,[1] E. Nava,[1] M. Rosas,[1] M. Fuenmayor,[1] I. M. González,[1] G. R. Meira,[2] H. M. Oliva[1]

[1]*Facultad de Ingeniería, Universidad del Zulia, Maracaibo, Venezuela*
[2]*Instituto de Desarrollo Tecnológico para la Industria Química (INTEC) (Consejo Nacional de Investigaciones Cientificas y Técnicas [CONICET] and Universidad Nacional del Litoral), Santa Fe 3000, Argentina*

Received 10 March 2003; accepted 24 September 2003

ABSTRACT: In this study, we investigated the synthesis of high-impact polystyrene through a series of (batch and bulk) polymerizations of styrene in the presence of 6 wt % polybutadiene. The reactions with rubber involved three stages: dissolution, prepolymerization, and finishing. The prepolymerizations were isothermal (at 70°C) and nonisothermal (with an initial heating period from 70 to 120°C). Purely thermal reactions were compared with chemically initiated polymerizations involving *tert*-butyl peroctoate (TBPO), 2,2′-azobisisobutyronitrile (AIBN), and their mixtures. Most prepolymerizations involved a stirring rate of 125 rpm. The particle morphology was mainly determined by the evolution of the grafting efficiency, stirring rate, and system viscosity during prepolymerization. In the nonisothermal prepolymerizations with pure AIBN, the grafting efficiency was lower than in equivalent prepolymerizations without an initiator, yielding unstable emulsions and a poor final morphology. In the nonisothermal prepolymerizations with pure TBPO, a large amount of graft copolymer was produced early in the prepolymerization, yielding a submicrometer core–shell morphology. The particle size and morphology could be controlled by the appropriate adjustment of the recipe and the prepolymerization conditions. © 2004 Wiley Periodicals, Inc. J Appl Polym Sci 92: 1397–1412, 2004

Key words: polystyrene; graft copolymers; TEM

INTRODUCTION

High-impact polystyrene (HIPS) has been produced through the bulk process for over 50 years. However, many details of its complex physical chemistry are still unknown and/or are a matter of controversy. An indication of the system complexity is that so far, no (heterogeneous) mathematical model of the process has been developed that is capable of predicting the evolution of the particle morphology. The general aim of this study was to further understand the complex interrelationships among particle morphology [and other intermediate structural variables, such as grafting efficiency and polystyrene (PS) molecular weights], prepolymerization conditions (temperature and stirring rate), and initiator capability of graft induction.

HIPS is a tough heterogeneous thermoplastic that consists of a continuous PS matrix containing dispersed rubber particles. Its physical properties are determined by variables such as molar mass, level of grafting, and particle morphology. The more standard HIPS grades exhibit salami-type morphologies, with particles in the range 1–3 μm, with smaller PS occlusions. Salami-type grades are typically produced by the dissolution of (a free-radically produced) polybutadiene (PB) into the styrene (St) monomer and then the polymerization of the monomer in the presence of a chemical initiator. Other typical reagents are a solvent and/or an oil for the reduction of system viscosity, an antioxidant for the prevention of rubber crosslinking, and a chain-transfer agent (normally a mercaptane) to reduce the PS chain lengths. Some special HIPS grades used for the production of translucent films with high surface gloss require submicrometer particles with core–shell morphologies. These (more expensive) grades can be produced by the simple blending (in the melt) of a PS homopolymer with a linear anionic (diblock or triblock) St–butadiene (Bd) copolymer. In this study, only the standard HIPS process that includes PB in the recipe was considered.

The bulk HIPS process can be either batch or continuous, and the following stages can be identified: dissolution, prepolymerization, finishing, and devola-

Correspondence to: H. M. Oliva (haydeeol@luz.ve).
Contract grant sponsor: Universidad del Zulia.
Contract grant sponsor: Consejo de Desarrollo Científico de y Humanístico de la Universidad del Zulia (CONDES-LUZ) (Venezuela)
Contract grant sponsor: Universidad del Litoral
Contract grant sponsor: Consejo Nacional de Investigaciones Científicas y Técnicas (CONICET) (Argentina)
Contract grant sponsor: Fondo Nacional de Ciencia, Tecnología e Innovación (FONACIT)-CONICET (international agreement).

tilization. In the dissolution stage, grated rubber is dissolved into the monomer at a relatively low temperature (50–70°C), to minimize thermal polymerization. The prepolymerization stage proceeds between 90 and 120°C under well-stirred conditions and generally in the presence of a chemical initiator. In a batch reaction, the system is homogeneous up to around 3% conversion, when a PS-rich phase begins to separate from the (continuous) PB-rich phase. The dispersed PS-rich phase grows in volume, and a phase inversion period takes place between 10 and 15% conversion. After the phase inversion, the number of rubber particles is fixed, and the PS–monomer solution remains as the continuous phase until the end of the reaction. The initiator half-life is selected such that the initiator is almost totally consumed during the prepolymerization stage. In the finishing stage, the polymerization proceeds with an increasing temperature, from around 30 to 75% conversion. During finishing, the free radicals are basically produced by thermal monomer decomposition, and the stirring is moderated to avoid destruction of the developed morphology. Finally, the reaction mixture is heated up to 230°C and devolatilized *in vacuo* to eliminate the solvent and residual monomer.

In the standard HIPS process, the generation of graft copolymer during the prepolymerization is vital because of its effect on morphology and mechanical properties. By accumulating at the interfaces, the graft copolymer reduces the interfacial tension, promotes the phase inversion, and controls the particle size.[1,2] The grafting efficiency is defined as the mass of grafted St divided by the total mass of polymerized St. For fixed stirring conditions, a high grafting efficiency at the beginning of the prepolymerization promotes an early phase inversion with the generation of small rubber particles. In contrast, a low level of grafting delays the phase inversion and generates large particles with a large dispersion in their diameters and occlusion diameters.

The complexity of the HIPS process results from the combination of several effects: (1) the polymerization proceeds in two immiscible liquid phases; (2) the mass transfer of reagents and products between phases is a function of many variables (which change along the reaction), such as temperature, viscosity, stirring rate, molar mass, grafting efficiency, and interfacial surface; and (3) the graft copolymer promotes a stable liquid–liquid dispersion, and it is extremely difficult (if not impossible) to determine the composition and molecular structure in each of the phases or subphases.

The grafting reactions initially involve the extraction of an allylic hydrogen of a Bd repeating unit by chain transfer from a monomeric radical, a polystyryl radical, or a primary initiator radical ($I^{\bullet}$).[3,4] The grafting kinetics have been investigated in several studies.[5–7] Compared to azo compounds such as 2,2′-azobisisobutyronitrile (AIBN), peroxide-type initiators such as benzoyl peroxide (BPO) or *tert*-butyl peroctoate (TBPO) are more effective in the induction of rubber grafting.[8–10] The performances of BPO and AIBN have been compared in several articles.[4,11–16] Despite its industrial importance, no published information could be found on the effect of TBPO on the HIPS morphology.

AIBN decomposes faster than BPO; for example, at 60°C, the half-lives of AIBN and BPO are 20 and 60 h, respectively. Huang and Sundberg[4,12,13] compared the performances of BPO and AIBN in independent homopolymerizations of St and benzyl methacrylate in the presence of PB. They concluded that although AIBN is almost incapable of inducing grafting, BPO generates grafting by the said allylic hydrogen mechanism. Ludwico and Rosen[14] investigated the effect of the dissolved PB on the polymerization rate of St initiated with BPO or AIBN. To minimize the problems of system heterogeneity and the gel effect, the reaction rates were measured at conversions lower than 1.5%. The polymerization rate slowed down with increasing values of the rubber mass or the rubber molar mass. Also, this reduction was more noticeable for BPO than AIBN.[14]

Kekhaiov and Mikhnev[15] compared a series of polymerizations of St in the presence of 5.8% of PB. The isothermal and bulk prepolymerizations were followed by a finishing stage that involved a suspension process. Two prepolymerizations were tested at 86°C with a chemical initiator and at 113°C with thermal initiation. The prepolymerizations at 86°C were carried out with different combinations of the initiators (BPO or AIBN) and the chain-transfer agent [*tert*-dodecyl mercaptane (*t*-DDM)]. The material produced with the highest contents of AIBN and *t*-DDM had large salami-type particles with large occlusions. In contrast, the material obtained with the highest concentration of BPO and the lowest concentration of *t*-DDM had small particles with small occlusions.

Riess and Gaillard[16] investigated the polymerization of St with PBs of different origins but of similar concentrations of 1,2-vinyl units. All of the prepolymerizations were isothermal at 70°C, and the following variables were modified: rubber contents, stirring rate, initiator nature (BPO or AIBN), and *t*-DDM concentration. The phase inversion was delayed to higher St conversions when the rubber concentration was increased with respect to a base value of 8 wt %. The stirring rates were 30, 50, and 80 rpm. At 30 rpm, the material exhibited an inadequate morphology, with PB filaments dispersed in a PS matrix. For the two faster speeds, the polymer exhibited the typical salami morphologies, but at 80 rpm, the rubber particles were smaller and had more uniform occlusions. With BPO,

the phase inversion was delayed to higher conversions with respect to AIBN, but the rubber particles were smaller and contained smaller occlusions. For increasing concentrations of AIBN and BPO, the particle diameters were also larger. However, although the BPO concentration did not affect the dispersion of the occlusion diameters, the occlusion diameters increased in size with increasing AIBN concentration. Finally, by augmentation of the *t*-DDM concentration, the phase inversion shifted toward higher conversions, with a sharp increase in particle size and occlusion sizes.[16]

The mentioned increase in particle size with the initiator concentration[16] was later verified by Estenoz et al.[17] when they compared the performances of TBPO and Lupersol-256 (a bifunctional initiator). A possible explanation is that the PS molecular weights were lowered by increasing initiator concentration, and this, in turn, reduced the system viscosity. The mentioned increase in particle size with the transfer agent concentration[16] can be explained as follows: (1) the transfer reactions lowered the grafting efficiency by shortening the grafted PS chains with no affect on the generation of grafting sites or the rate of polymerization, and (2) the mass of occluded PS increased when the PS chain lengths were reduced.[18] This last effect was supported by the following observation: when a low-molecular-weight PS was added onto the reaction mixture before the phase inversion, there was an increase in the size and number of the particle occlusions.

Peng[19] and Demirrors et al.[20] aimed to control the average number of branches per copolymer molecule (and, therefore, interfacial tension) by replacing the standard PB for hydroperoxide-terminated PBs. To this effect, standard PB was first functionalized by a reaction with an oxygen singlet. The resulting morphologies were similar to those produced when with linear diblock or triblock St–Bd copolymers.

Fischer and Hellman[18] correlated the average number of grafted PS branches per copolymer molecule with the developed morphologies. They compared the morphology obtained after a simple devolatilization of the reaction mixture with the equivalent thermodynamically controlled morphology. This last morphology was obtained by the isolation of the polymer (by precipitation in methanol), redissolution of the polymer in toluene, and production of a thin polymeric film by slow solvent evaporation. They concluded that the thermodynamic phase inversion occurred when the copolymer exhibited an average of two grafted PS chains per molecule. Copolymer molecules with two or more PS branches placed themselves at the external interface of the particles, whereas copolymer molecules with a single PS branch placed themselves at the occlusion interface.[18]

This study could be considered a continuation of that of Riess and Gaillard.[16] In this article, a series of nonisothermal prepolymerizations with a final temperature of 120°C and different AIBN–TBPO mixtures are described. These results are compared with equivalent isothermal prepolymerizations at 70°C, purely thermal polymerizations, and St homopolymerizations without rubber.

EXPERIMENTAL

Polymerizations

The left-hand side of Table I presents the main experimental conditions. In the main set of experiments (1–12), a fixed 6 wt % PB with respect to the monomer was used, whereas experiments A–H were carried out without rubber. The aim of experiments A–H was to determine the evolution of the St conversion and the PS molecular weights along the prepolymerizations in similar conditions to the main reactions. To isolate purely thermal effects, experiments A, B, 1, and 2 were carried out without any initiator. In all of the experiments involving chemical initiators, the total initiator concentration was 0.003*M*. Pure AIBN, pure TBPO, and their mixtures were tested. All of the reactions included 10 vol % ethyl benzene with respect to the monomer, and 0.1 wt % antioxidant.

All of the experiments with rubber involved the following steps: (1) a 3-h dissolution stage at 70°C at a stirring rate of 250 rpm, (2) a stirred prepolymerization that was stopped when the monomer conversion was close to 35%, and (3) an unstirred finishing stage at 150°C lasting 12 h. The reactions without rubber also included a dissolution stage but excluded the finishing stage.

In experiments A, C, E, G, 1, 3, 5, 7, and 9–12, the prepolymerizations were isothermal at 70°C. In experiments B, D, F, H, 2, 4, 6, and 8, the prepolymerizations were nonisothermal with an initial heating period from 70°C at 1°C/min, followed by an isothermal period at 120°C. In the prepolymerizations without rubber, the stirring rate was relatively high (250 rpm). In most of the prepolymerizations with rubber, the basic stirring rate was 125 rpm, but rates of 250 and 375 rpm were also tested.

The following reagents were used: (1) St from Chevron (St. James, LA), (2) Intene medium *cis*-PB (40% 1,4-*cis*-PB, 50% 1,4-*trans*-PB, and 10% 1,2-vinyl-PB) from Enichem (Italy), (3) AIBN (Perkadox) from Akzo (Sao Paulo, Brazil), (4) TBPO from Akzo, (5) ethyl benzene from E. M. Science (Darmstadt, Germany), and (6) a Polygard mixture of di/trinonyl-phenyl-phosphite and triisopropyl alcohol amine from Uniroyal (Middlebury, CT) as an antioxidant. All of the reagents were used as received with the exception of

TABLE I
Recipes, Prepolymerization Conditions, and Global Results

	Recipe			Prepolymerization conditions		Prepolymerization results					Particle morphology	
		Initiators mixture (molar concentration)										
Experiment	PB concentration (phm)[a]	AIBN (%)	TBPO (%)	Temperature (°C)	Stirring rate (rpm)	St conversion (%)	Grafting efficiency (%)	$M_{n,PS}$ (g/mol)	$M_{w,PS}$ (g/mol)	$M_{w,PS}/M_{n,PS}$	D_v (μm)[b]	TEM
A	—	—	—	70	250	17	—	600,000	1,080,000	1.80	—	—
B	—	—	—	120[c]	250	21	—	208,000	410,000	1.97	—	—
C	—	100	0	70	250	10	—	30,000	271,000	9.03	—	—
D	—	100	0	120[c]	250	20	—	72,000	160,000	2.22	—	—
E	—	0	100	70	250	19	—	215,000	460,000	2.14	—	—
F	—	0	100	120[c]	250	25	—	75,000	160,000	2.13	—	—
G	—	50	50	70	250	21	—	132,000	250,000	1.89	—	—
H	—	50	50	120[c]	250	21	—	68,000	131,000	1.93	—	—
1	6	—	—	70	125	19	16.8	179,000	453,000	2.53	2.05	Figure 4
2	6	—	—	120[c]	125	13	20.4	162,000	332,000	2.05		
						21	19.0	156,000	346,000	2.22	[d]	Figure 5
3	6	100	0	70	125	20	13.0	128,000	256,000	2.00	5.84	Figure 6
4	6	100	0	120[c]	125	17	12.1	50,000	97,100	1.94		
						26	15.3	63,000	138,000	2.19	[e]	Figure 7
5	6	0	100	70	125	20	23.2	163,000	323,000	1.98	1.48	Figure 8
6	6	0	100	120[c]	125	13	24.6	56,000	100,000	1.79		
						18	24.2	51,000	95,100	1.86	1.30	Figure 9
7	6	50	50	70	125	20	13.1	112,000	227,000	2.03	2.53	Figure 10
8	6	50	50	120[c]	125	17	16.0	45,000	100,000	2.22		
						25	17.0	69,000	138,000	2.00	2.60	Figure 11
9	6	50	50	70	250	21	14.8	113,000	222,000	1.96	1.53	Figure 12
10	6	50	50	70	375	20	16.9	137,000	253,000	1.85	1.37	Figure 13
11	6	25	75	70	125	21	[d]	133,000	247,000	1.86	2.04	Figure 14
12	6	75	25	70	125	20	[d]	115,000	212,000	1.84	3.42	

[a] Parts per hundred monomer (weight).
[b] Volume-based average particle diameter of the final polymer.
[c] With a 50 min initial heating period at 1°C/min from 70 to 120°C.
[d] Rejected measurement.
[e] Unmeasurable PSD (before phase inversion).

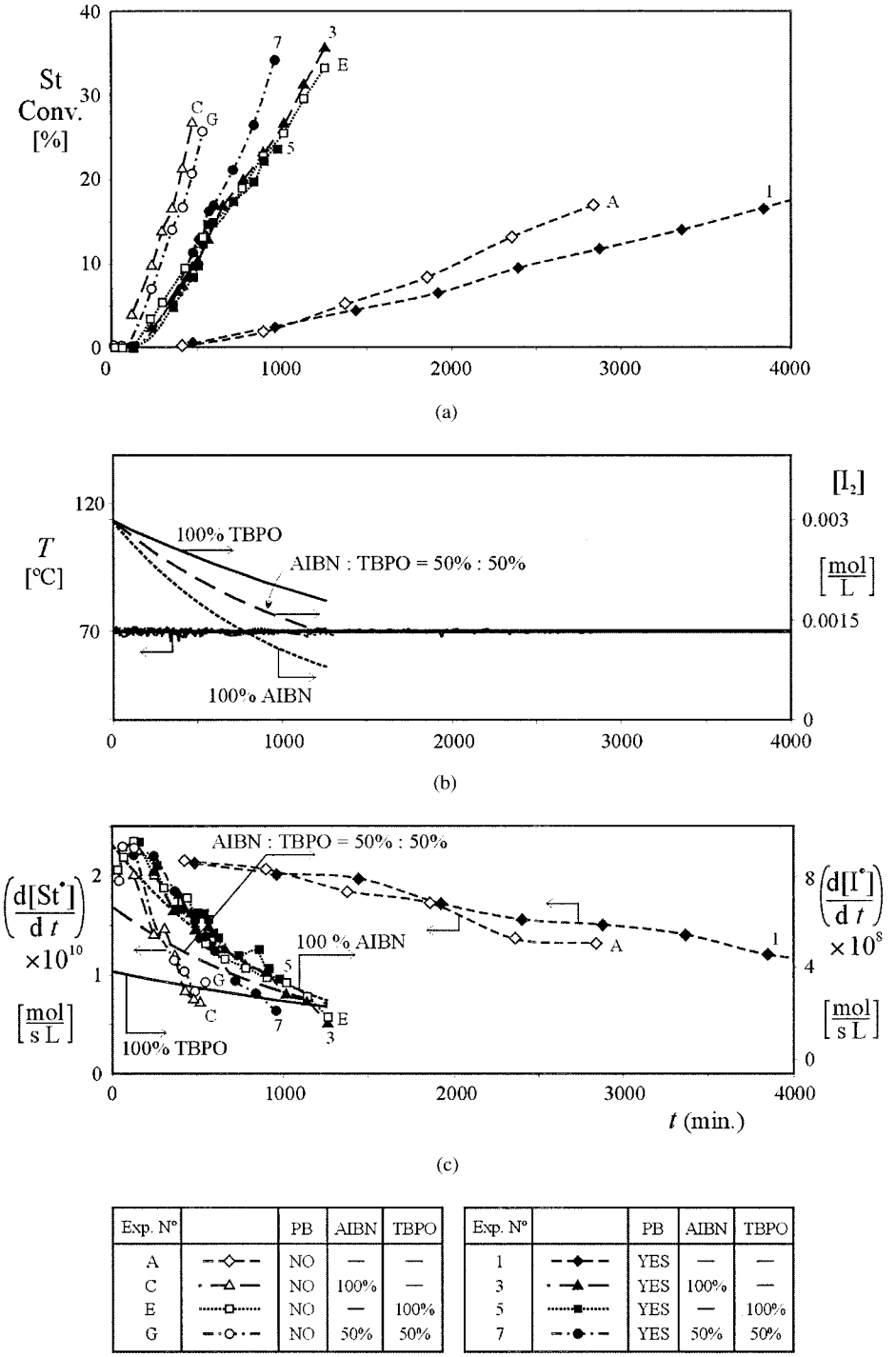

Exp. N°		PB	AIBN	TBPO
A		NO	—	—
C		NO	100%	—
E		NO	—	100%
G		NO	50%	50%

Exp. N°		PB	AIBN	TBPO
1		YES	—	—
3		YES	100%	—
5		YES	—	100%
7		YES	50%	50%

Figure 1 Isothermal prepolymerizations at 70°C (experiments A, C, E, G, 1, 3, 5, and 7): (a) St conversion; (b) desired temperature (solid line), measured temperatures (traced lines), and theoretical concentration of the total initiator for pure TBPO, pure AIBN, and their 50:50 mixture; and (c) estimated rate of generation of monomeric and initiator free radicals.

AIBN, which was recrystallized in ethanol. To emulate industrial conditions, the stabilizer, a catechol, was not eliminated from the monomer; it was assumed that the stabilizer was mostly consumed during the thermal dissolution.

The dissolution and prepolymerization stages were carried out in a 2-L stainless steel reactor from Büchi Glassuster (Uster, Switzerland). The reactor contained a single 45° turbine stirrer fit at the shaft end. The reactions were all carried out under nitrogen. Except for the initiators (which were added at the beginning of the prepolymerization), all of the reagents were loaded at the beginning of the dissolution stage. The temperature was manually controlled by the manipu-

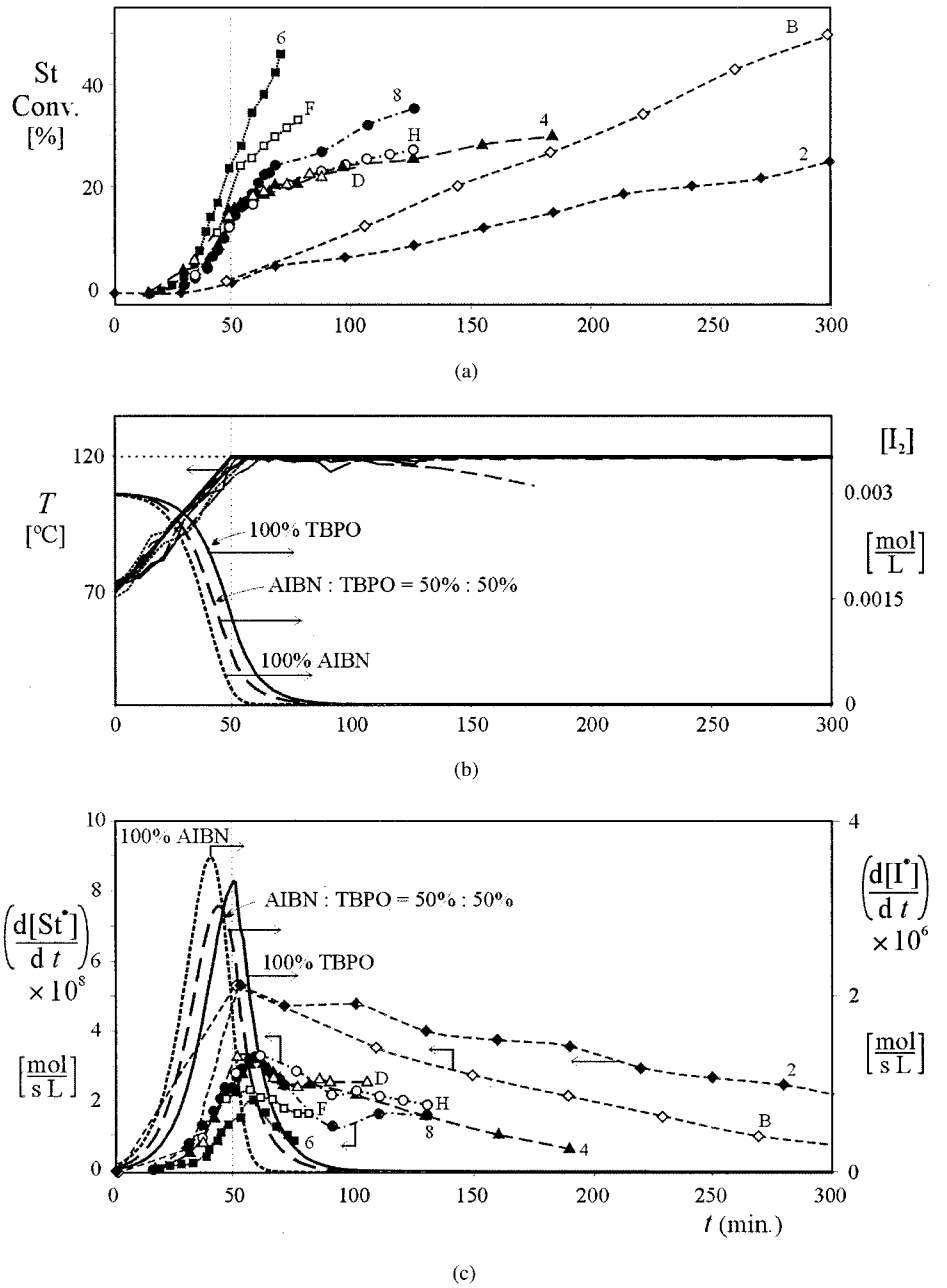

Exp. N°		PB	AIBN	TBPO
B		NO	—	—
D		NO	100%	—
F		NO	—	100%
H		NO	50%	50%

Exp. N°		PB	AIBN	TBPO
2		YES	—	—
4		YES	100%	—
6		YES	—	100%
8		YES	50%	50%

Figure 2 Nonisothermal high-temperature prepolymerizations (experiments B, D, F, H, 2, 4, 6, and 8): (a) St conversion; (b) desired temperature (solid line), measured temperatures (traced lines), and theoretical concentration of the total initiator for pure TBPO, pure AIBN, and their 50:50 mixture; and (c) estimated rate of generation of monomeric and initiator free radicals.

lation of two temperatures, that of an external heating bath and that of an internal cooler (which also served as a baffle). In the low-temperature prepolymerizations, the reaction temperature fluctuated moderately around 70°C [see the cloud of measured temperatures in Fig. 1(b)]. In the nonisothermal experiments, relatively larger deviations with respect to the desired temperature profile were observed [Fig. 2(b)].

Along the prepolymerizations, the solid contents were gravimetrically determined as follows: (1) a film

of the reaction mixture was formed on an aluminum plate, and (2) the solvent and residual monomer were evaporated by means of a heating lamp. This allowed a rough online determination of conversion and, therefore, of the end of the prepolymerization. For the finishing stage, part of the reaction mixture was transferred (via a vacuum pump) into U-shaped glass ampules with an internal diameter of 5 mm. These ampules were then sealed, maintained at 150°C for 12 h, and finally broken for analysis of the final morphology. Even though the final conversions were not measured, they were thought to be all above 97%.

Offline measurements

Several analyses were carried out as the samples were undergoing prepolymerization. First, the total polymer was isolated from the unreacted reagents by precipitation in methanol. Then, the precipitate was filtered, dried *in vacuo* at room temperature, and weighed. The monomer conversion was obtained by subtraction of the original PB weight from the weight of the dry polymer. For the samples taken near 20% conversion, the free PS was extracted from the total dry polymer and analyzed by size exclusion chromatography (SEC). The PS was isolated with a three-stage solvent extraction procedure involving a 50:50 mixture of methyl ethyl ketone (MEK)/dimethylformamide.[6] The grafting efficiency was calculated from the values of monomer conversion and undissolved polymer mass (graft copolymer + residual PB). This technique is known to provide values in excess because of the difficulty of quantitatively extracting the free PS contained in the particle occlusions.[6] The molecular weights of the free PSs were measured in a Waters 244 ALC/GPC size exclusion chromatograph (Milford, MA) fit with a complete set of μ-styragel columns (with nominal pores of 100, 500, 10^3, 10^4, 10^5, and 10^6 Å).

For fixed values of the monomer conversion, stirring rate, and temperature, the global viscosity was determined by the nature of the continuous phase. During the phase inversion, the viscosity dropped despite the continuous increase in conversion. This was justified as follows. After the initial homogeneous period, the monomer was almost evenly partitioned between the two phases. The molar mass of the initial PB was generally larger than the molar mass of the free PS, and the largest molecular weights corresponded to the graft copolymer (which was almost exclusively produced in the PB-rich phase). Before the phase inversion, the viscosity was relatively high because the PB-rich phase was the continuous phase. During the phase inversion, the viscosity dropped because the PS-rich phase became the continuous phase. The viscosity of some selected prepolymerization samples was determined through a Brookfield viscometer (DV-I model; Stoughton, MA). These measurements were carried out at 26°C.

In each of the experiments with rubber, two samples were taken to analyze their morphology by transmission electron microscopy (TEM; Phillips EM 201; Eindhoven, The Netherlands). The first sample was taken at the end of prepolymerization, and it was pretreated at room temperature to eliminate the solvent and residual monomer (and to this effect, a high vacuum was applied to a film of the final prepolymer). The second sample corresponded to the final polymer, and it was analyzed as such, without elimination of the low molar mass material. For the TEM analyses, the sample preparation involved the cutting of the solids into ultrafine sections and the dyeing of the PB chains with OsO_4.

Average particle diameters could not be simply determined by TEM. The reasons were that (1) a large number of particles had to be counted and sized and (2) the observed particle slices were randomly cut at different levels, and therefore, their diameters were in general smaller than the true particle diameters. Instead, a centrifugal sedimentometer (Horiba Capa-700; Irvine, CA) was used to estimate the mass-based (or volume-based) particle size distribution (PSD) of the final polymer. Then, the volume-based average diameter was calculated from such distribution. The sample preparation simply involved the dispersion of 0.1 g of the solid into 14 mL of MEK. The main assumption was that the solvent only dissolved the continuous (PS-rich) phase without affecting the particle size. Note that a volume-average diameter is always larger than the corresponding number-average value.

RESULTS AND DISCUSSION

The global results are presented in the right-hand side of Table I. The following values are given: (1) the grafting efficiency, the average molecular weights and polydispersity of the free PS ($M_{w,PS}/M_{n,PS}$, where $M_{w,PS}$ is the weight-average molecular weight of polystyrene and $M_{n,PS}$ is the number-average molecular weight of polystyrene) determined at a conversion close to 20% and (2) the volume-based average diameter of the final sample. For the main experiments 2, 4, 6, and 8, the grafting efficiencies and molecular weights at a conversion close to 10% are also presented.

Figure 1 corresponds to the isothermal (low-temperature) prepolymerizations of experiments A, C, E, G, 1, 3, 5, and 7; whereas Figure 2 corresponds to the nonisothermal (high-temperature) prepolymerizations of experiments B, D, F, H, 2, 4, 6, and 8. Figures 1(a) and 2(a) represent the evolution of the monomer conversion; and the last point of each plot corresponds to the prepolymerization end sample (which was later

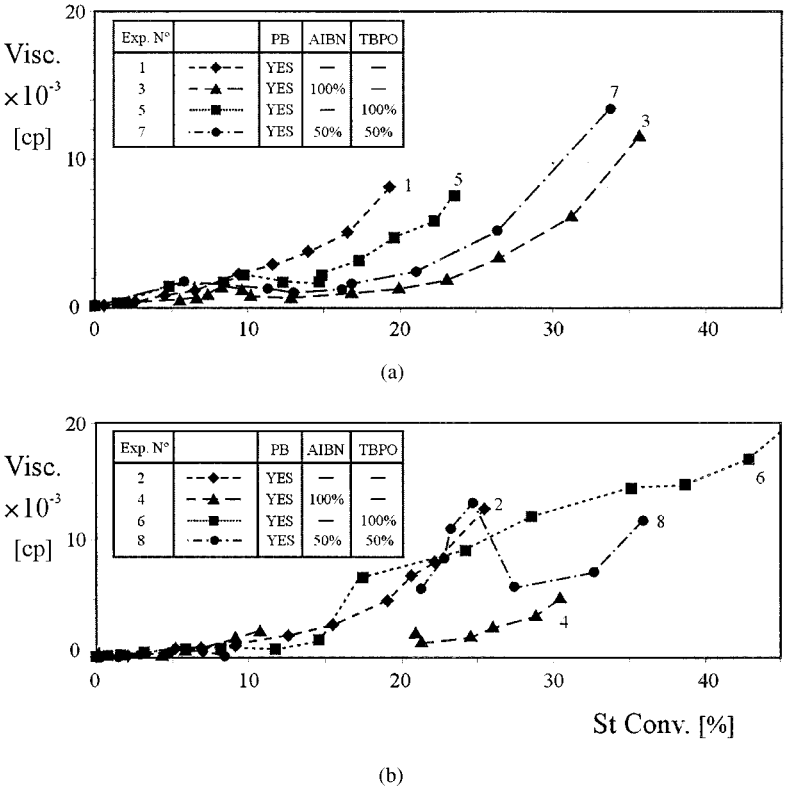

Figure 3 Brookfield viscosity versus St conversion for the reactions with rubber at 125 rpm: (a) isothermal experiments 1, 3, 5, and 7 and (b) nonisothermal experiments 2, 4, 6, 8. In experiments 4 and 8, viscosity measurements could not be done between 10 and 20% conversion because of a demixing of the liquid–liquid dispersion. For this reason, curves 4 and 8 in are shown as discontinuous in that range.

analyzed by TEM). Figures 1 and 2 present the prepolymerizations carried out with the following AIBN to TBPO molar ratios: 0:0, 100:0, 50:50, and 0:100. For experiments 1–8 (carried out with rubber at 125 rpm), the sample viscosities were measured and plotted versus the monomer conversion [Fig. 3(a,b)]. In experiments 11 and 12, the initiator ratios were 25:75 and 75:25. Experiments 9 and 10 were carried out with stirring rates of 250 and 375 rpm, respectively.

The morphologies of experiments 1–11 are given in Figures 4–14. In these figures, the final sample micrograph is presented under the first part, the final sample PSD is presented under the second part (except in Fig. 5, where the PSD is missing), and the micrograph of the prepolymerization end sample is presented under the third part. Not all of this information is given in Figures 4–14 (e.g., in Fig. 5, the PSD is missing).

In general, the final polymer micrographs [Figs. 4(a)–14(a)] showed more particle deformation (because of the cutting process) than the prepolymerization end micrographs [Figs. 4(c)–14(c)]. There were two reasons for this: (1) the solvent and residual monomer were not eliminated from the final TEM samples, and (2) the temperature of the finishing stage determined that the final PS molecular weights (not presented in this article) were lower than the PS molecular weights at the prepolymerization end. Thus, the continuous phase of the final material was softer than the continuous phase of the prepolymerization end sample. Also, the occlusions of the final samples were larger than the occlusions of the prepolymerization end samples. An explanation for this was that the low-molecular-weight PS produced during the finishing stage tended to accumulate in the occlusions.

Before we analyze the results further, we present the estimation of the rate of generation of chemical and thermal free radicals during the prepolymerizations.

Generation of free radicals

I•'s are produced from

$$I_2 \xrightarrow{k_{d,I}} 2I^{\bullet}$$

where I_2 is either AIBN or TBPO and $K_{d,I}$ is the initiator decomposition constant. The molar concentration of unreacted initiator is given by

$$\frac{d}{dt}[I_2(t)] = -k_{d,I}(T)[I_2(t)] \quad (1)$$

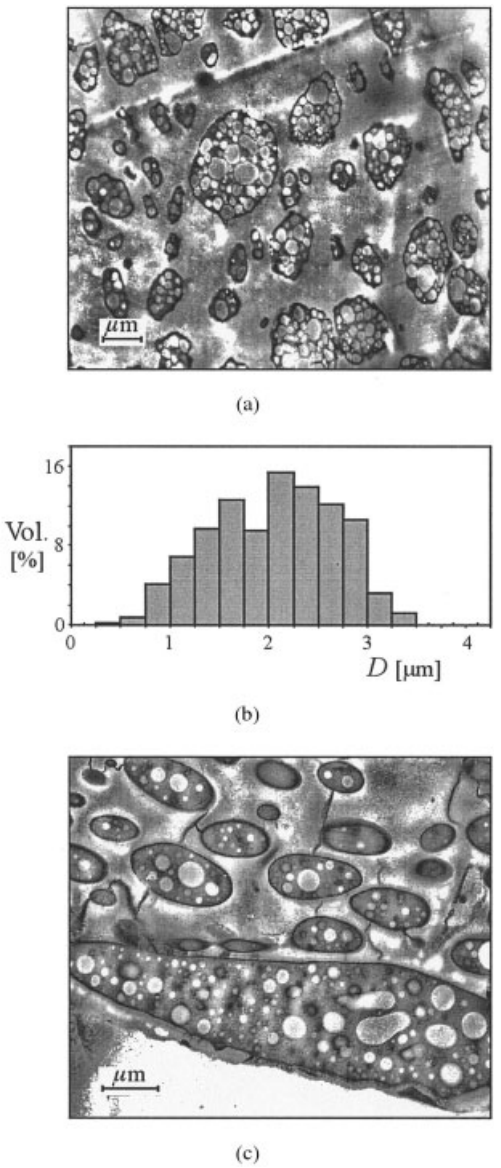

Figure 4 Morphology of experiment 1 (no initiator, low-temperature prepolymerization at 125 rpm): (a,b) final polymer and (c) polymer at the end of prepolymerization.

with $k_{d,\mathrm{AIBN}}(T) = 1.5379 \times 10^{15} \times e^{-15548/T}$ (s^{-1})[21] and $k_{d,\mathrm{TBPO}}(T) = 9.117 \times 10^{13} \times e^{-14888/T}$ (s^{-1}).[21]

Equation (1) was integrated with the assumption of the desired (or nominal) temperature profiles [$T(t)$, where T is the temperature and t is the time], represented by a bold continuous trace in Figures 1(b) and 2(b). The numerical solutions are also shown in Figures 1(b) and 2(b). The curves identified with 100% AIBN apply to experiments C, D, 3, and 4; those identified with 100% TBPO apply to experiments E, F, 5, and 6; and those identified with AIBN/TBPO = 50:50 apply to experiments G, H, 7, and 8. AIBN decomposed more rapidly than TBPO. In the case of the initiator mixture, the total initiator concentration was intermediate between the pure AIBN and pure TBPO cases. In the prepolymerizations at 70°C, the initiators decomposed throughout this stage, and a high initiator concentration remained at the prepolymerization end. In the high-temperature prepolymerizations, the initiators were mostly consumed during the heating period.

The total rate of generation of initiator free radicals was calculated by the injection of the composition profiles of Figures 1(b) and 2(b) into the right-hand side of the following equation:

$$\frac{d}{dt}[\mathrm{I}(t)^{\cdot}] = 2f_{\mathrm{AIBN}}k_{d,\mathrm{AIBN}}(T)[\mathrm{AIBN}(t)] + 2f_{\mathrm{TBPO}}k_{d,\mathrm{TBPO}}(T)[\mathrm{TBPO}(t)] \quad (2)$$

with the efficiency factors arbitrarily chosen as follows: $f = f_{\mathrm{AIBN}} = f_{\mathrm{TBPO}} = 0.5$. The resulting rates were the smooth curves indicated by 100% AIBN, 100% TBPO, and AIBN/TBPO = 50:50 in Figures 1(c) and 2(c).

The thermal monomer decomposition is represented by

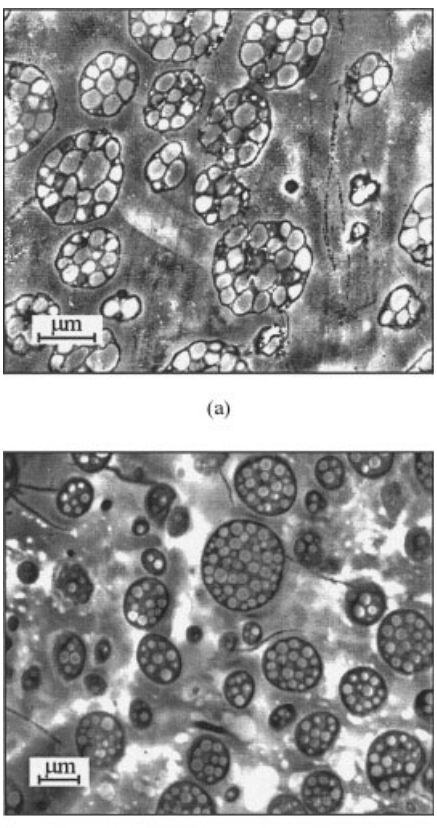

Figure 5 Morphology of experiment 2 (no initiator, high-temperature prepolymerization at 125 rpm): (a) final polymer and (b) polymer at the end of prepolymerization.

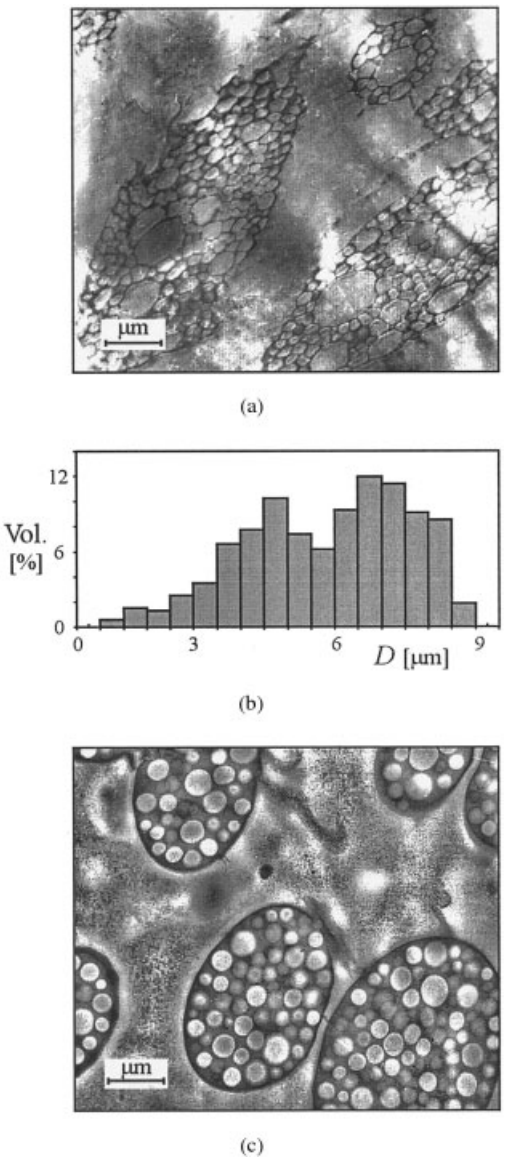

Figure 6 Morphology of experiment 3 (pure AIBN, low-temperature prepolymerization at 125 rpm): (a,b) final polymer and (c) polymer at the end of prepolymerization.

$$3\mathrm{St} \xrightarrow{k_{d,\mathrm{St}}} 2\mathrm{St}$$

The rate of generation of thermal monomeric free radicals (which did not include the monomeric free radicals generated by chain transfer to the monomer) was directly estimated from the right-hand side of the following equation:

$$\frac{d}{dt}[\mathrm{St}(t)] = 2k_{d,\mathrm{St}}(T)[\mathrm{St}(t)^{\bullet}]^3 \qquad (3)$$

where $k_{d,\mathrm{St}}(T) = 2.1 \times 10^5 \times e^{-15000/T}$ ($\mathrm{L}^2\ \mathrm{mol}^{-2}\ \mathrm{s}^{-1}$).[6,19,21–24] For each experiment, the measured temperature was injected into $k_{d,\mathrm{St}}(T)$, and [St(t)] was determined from the conversion profiles of Figures 1(a) and 2(a). Figure 1(c) presents the generation rate of monomeric free radicals of experiments A, C, E, G, 1, 3, 5, and 7, and similarly, Figure 2(c) presents the generation rate of monomeric free radicals of experiments B, D, F, H, 2, 4, 6, and 8. As expected, the curves were highly oscillatory compared with the smooth theoretical predictions for the chemical initiators.

For the isothermal prepolymerizations, Figure 1(c) suggests that although the rate of generation of initiator free radicals was around 10^{-8} mol s^{-1} L^{-1}, the rate of generation of thermal free radicals was about two orders of magnitude lower. When Figures 1(c) and 2(c) are compared, one can see that (at 120°C), the

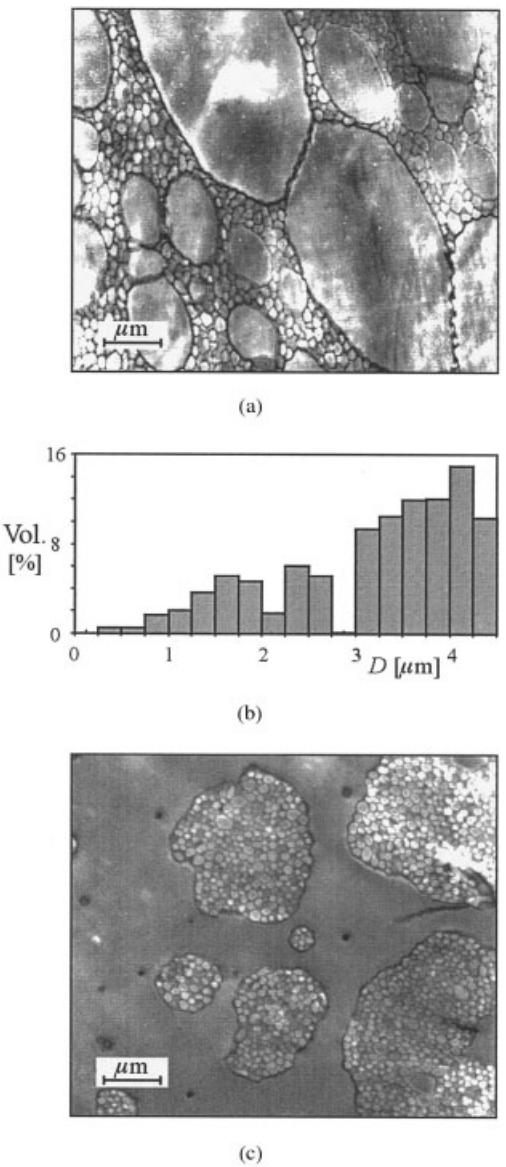

Figure 7 Morphology of experiment 4 (pure AIBN, high-temperature prepolymerization at 125 rpm): (a,b) final polymer and (c) polymer at the end of prepolymerization.

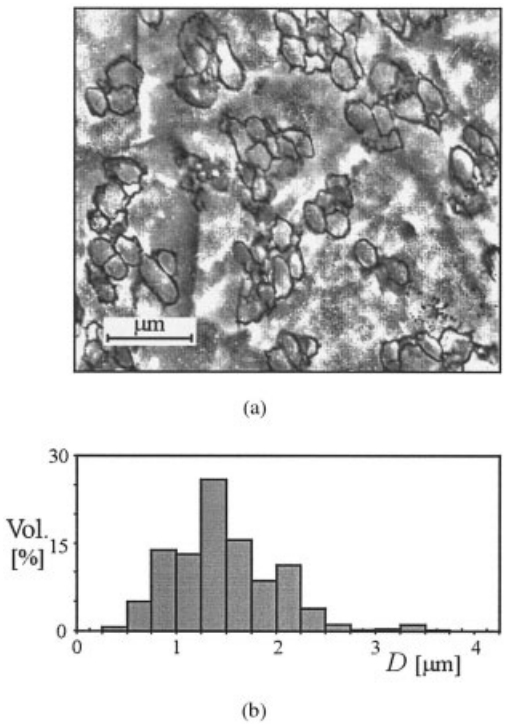

Figure 8 Morphology of experiment 5 (pure TBPO, low-temperature prepolymerization at 125 rpm): (a,b) final polymer.

generation rates were about two orders of magnitude higher than at 70°C. However, although the low-temperature prepolymerizations were dominated by chemical initiation, in some of the high-temperature prepolymerizations, the initiators were almost totally consumed at the prepolymerization end, and thereafter, the initiation was purely thermal [Fig. 2(c)].

Polymerizations without rubber (experiments A–H)

The results of the homogeneous experiments A–H are given in Table I and Figures 1 and 2. Independently of temperature, the rate of generation of initiator free radicals was about two orders of magnitude higher than the rate of generation of thermal monomeric free radicals [Figs. 1(c) and 2(c)]. Thus, the lowest polymerization rates and longest induction times were observed in the purely thermal reactions [in Fig. 1(a), cf. experiment A with experiments C, E, and G; in Fig. 1(b), cf. experiment B with experiments D, F, and H]. The induction periods were possibly caused by the stabilizer and/or by the oxygen that may have been dissolved in the monomer. Also, it has been suggested that the antioxidant can exhibit an induction behavior with the generation of inactive products.[25] Induction periods became longer for decreasing polymerization rates. This was reasonable because a fixed quantity of free radicals was required for the deactivation of a fixed amount of impurities in the monomer feed.

Consider the isothermal prepolymerizations of Figure 1. In the presence of initiator (experiments C, E, and G), the rates of polymerization increased in the order 100% TBPO < (AIBN/TBPO = 50:50) < 100% AIBN. The high-temperature prepolymerization results are given in Figure 2. In this case, the total reaction times were reduced by an order of magnitude with respect to the isothermal case. However, the relative reduction in reaction time was not as large as the relative reduction in the concentration of free radicals. The reason was that the chemical initiators were almost totally consumed after about 120 min. The applied temperature profiles determined a change in the conversion slopes at $t = 50$ min [Fig. 2(a)].

Consider the PS molecular weights of experiments A and B. In experiment A at 70°C, most of the PS was

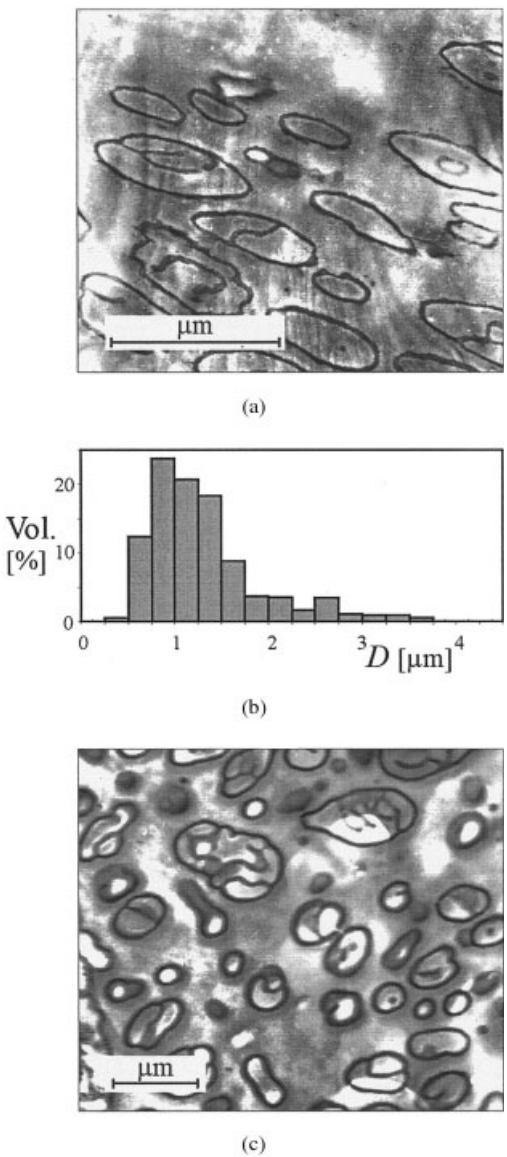

Figure 9 Morphology of experiment 6 (pure TBPO, high-temperature prepolymerization at 125 rpm): (a,b) final polymer and (c) polymer at the end of prepolymerization.

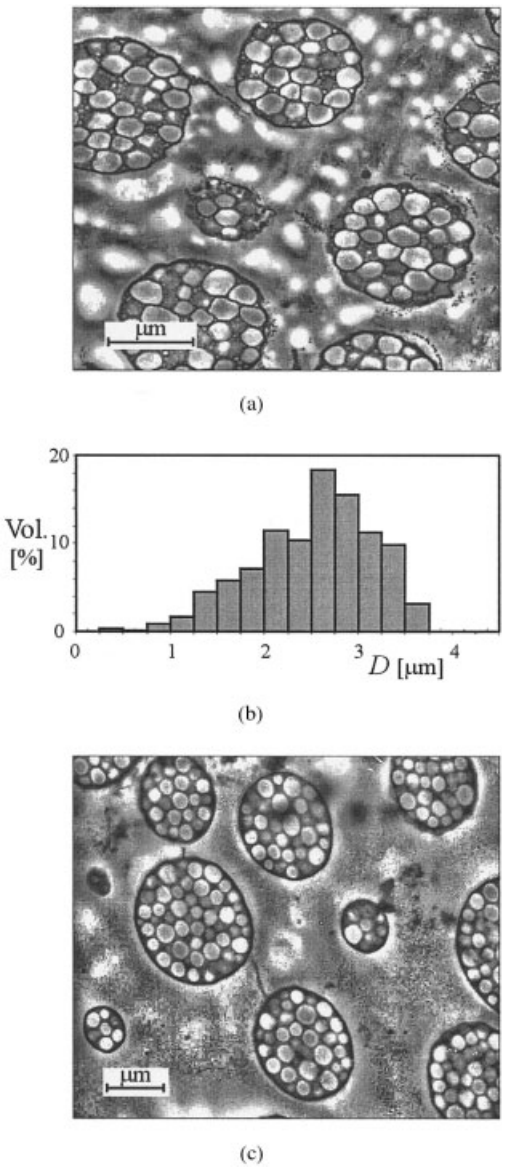

Figure 10 Morphology of experiment 7 (AIBN/TBPO = 50:50, low-temperature prepolymerization at 125 rpm): (a,b) final polymer and (c) polymer at the end of prepolymerization.

generated by recombination termination, and there was an almost constant generation of free radicals [curve A in Fig. 1(c)]. This yielded the highest molecular weights and the lowest $M_{w,PS}/M_{n,PS}$ values. (For a pure recombination termination, the instantaneous $M_{w,PS}/M_{n,PS}$ is 1.5.[6]) In experiment B, there was a significant drop in the PS molecular weights with respect to experiment A. At 120°C, most of the growing polystyryl radicals terminated by chain transfer to the monomer. This yielded a most probable instantaneous molecular weight distribution (MWD) of $M_{w,PS}/M_{n,PS} = 2$. Thus, an important drop in the instantaneous molecular weights was expected along the heating period, which justified the increase in $M_{w,PS}/M_{n,PS}$ of experiment B with respect to experiment A.

Initiators lowered the PS molecular weights with respect to equivalent initiator-free reactions. Also, the molecular weights were lower with AIBN than with TBPO because of the higher decomposition rate of the former (cf. experiment A with experiments C, E, and G; and cf. experiment B with experiments D, F, and H). The $M_{n,PS}$ value of experiment C was unexpectedly low, yielding an inexplicably high $M_{w,PS}/M_{n,PS}$. The molecular weights of experiments D, F, and H were all quite similar to each other because (independently of

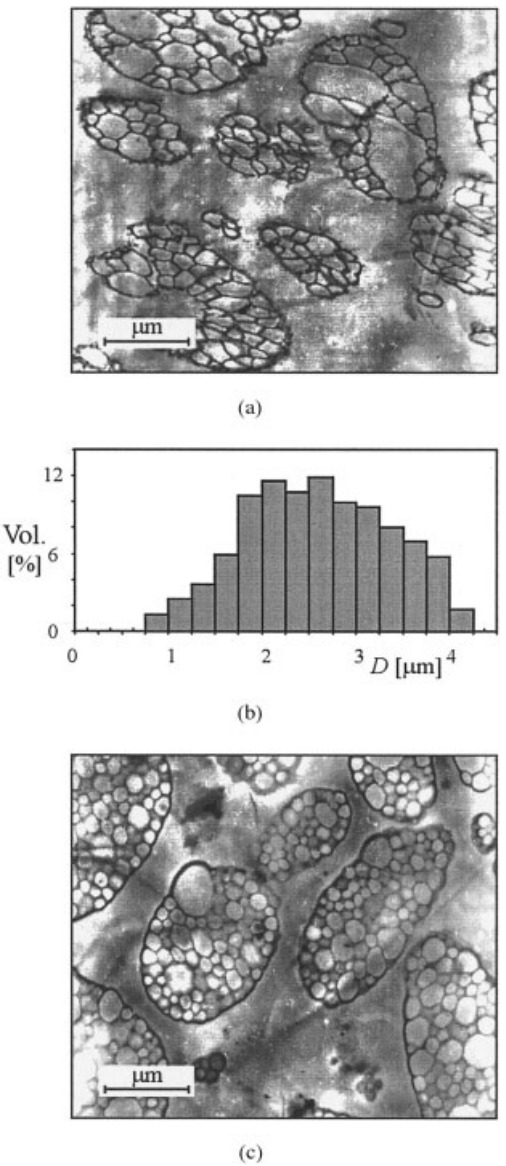

Figure 11 Morphology of experiment 8 (AIBN/TBPO = 50:50, high-temperature prepolymerization at 125 rpm): (a,b) final polymer and (c) polymer at the end of prepolymerization.

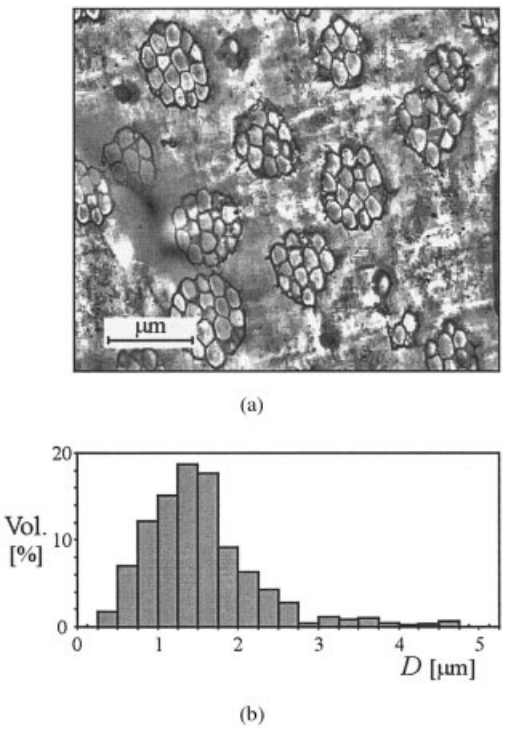

Figure 12 Morphology of experiment 9 (AIBN/TBPO = 50:50, low-temperature prepolymerization at 250 rpm): (a,b) final polymer.

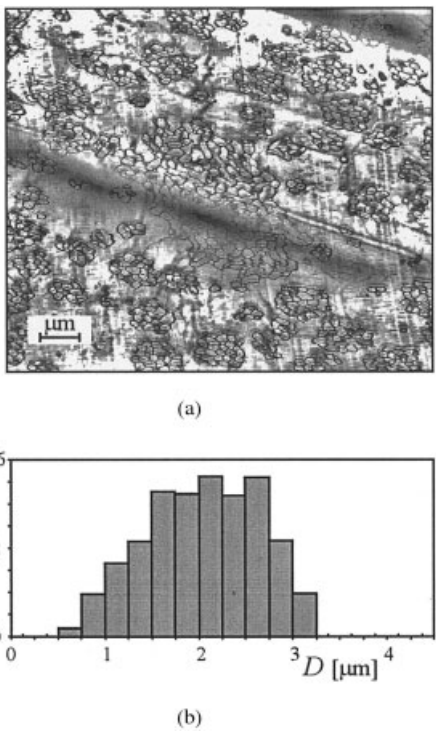

Figure 14 Morphology of experiment 11 (AIBN/TBPO = 25:75, low-temperature prepolymerization at 125 rpm): (a,b) final polymer.

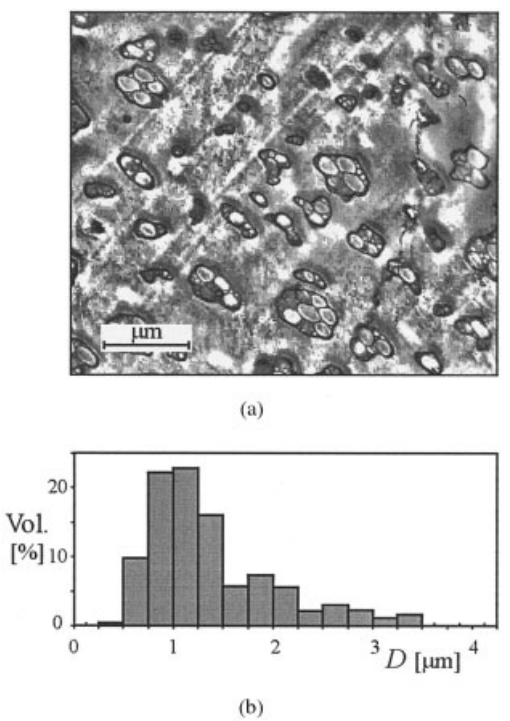

Figure 13 Morphology of experiment 10 (AIBN/TBPO = 50:50, low-temperature prepolymerization at 375 rpm): (a,b) final polymer.

the initiator nature), all of the initiator was consumed during the high-temperature prepolymerizations.

Polymerizations with rubber but without initiator (experiments 1 and 2)

In the absence of initiator, the (heterogeneous) thermal polymerizations were slowed down by the presence of rubber (cf. experiment 1 with experiment A, and cf. experiment 2 with experiment B). The polymerization in the PS-rich phase was similar to the equivalent rubber-free homopolymerizations. Thus, the slower rates in the presence of rubber were caused by the rubber-rich phase. This has been explained as follows: (1) primary rubber radicals are more stable than polystyryl radicals,[26] and (2) in the thermodynamically poorer PB-rich phase, there is a reduced gel effect by a shrinking of the growing macroradicals (which maintain a relatively high diffusivity and can, therefore, terminate more rapidly).[14]

In the rubber-free experiments, the following reactions generated dead PS: chain transfer to the monomer and recombination termination. In the presence of rubber, a third termination reaction was incorporated: chain transfer to the rubber. This explained the dramatic drop in the PS molecular weights and the increase in $M_{w,PS}/M_{n,PS}$ when experiment A is compared with experiment 1. The activation energies of the mentioned reactions were recombination termina-

tion = 1667 cal/mol,[27] transfer to the monomer = 14,400 cal/mol,[21] and transfer to the rubber = 18,000 cal/mol.[28] When the temperature was increased from 70 to 120°C, the rate of recombination termination only increased by a factor of 2, whereas the transfer to the monomer increased by a factor of 500, and the transfer to the rubber increased by a factor of 1000. When experiments 2 and B were compared, a drop in the molecular weights was observed with an increase in $M_{w,PS}/M_{n,PS}$. However, these changes were considerably less dramatic than in the low-temperature case. The reason was that both transfer reactions yielded the same instantaneous MWD, with the transfer to the monomer being dominant.

Free PS was produced in both phases, and there were varying conditions in each of the phases. For this reason, the $M_{w,PS}/M_{n,PS}$ values of the global PS produced in experiments 1 and 2 were larger than those of the equivalent homogeneous experiments A and B. For the same reason, the mathematical models that assume the bulk HIPS process as homogeneous systematically underestimated the global $M_{w,PS}/M_{n,PS}$.[6,28]

In the initiator-free polymerizations with rubber, the grafting reactions mostly occurred in the PB-rich phase by chain transfer to the rubber from the polystyryl radicals. The grafting efficiency of experiment 2 was higher than that of experiment 1; and this was reasonable if the difference in activation energies of the mentioned transfer reactions is considered. The viscosity plots of experiments 1 and 2 (Fig. 3) do not exhibit a minimum because the phase inversion may not have yet occurred at the (relatively low) conversions observed at the ends of prepolymerization (19 and 21%, respectively). Another possible reason is that the viscosity samples may have been taken too far apart for the detection a minimum. Also, the higher viscosities of experiment 1 with respect to 3, 5, and 7 [Fig. 3(a)] were a consequence of the higher PS molecular weights of experiment 1 compared with experiments 3, 5, and 7.

The particle morphologies are presented in Figures 4 and 5. Consider the (prepolymerization end) micrograph of Figure 4(c). Its upper section confirms the phase inversion, whereas its lower section indicates that the inversion had not yet occurred. In contrast, Figure 5(b) indicates that the system had already phase inverted. The final morphologies are given in Figures 4(a,b) and 5(a). Unfortunately, the PSD of experiment 2 was not measured by sedimentometry. However (as expected from the difference in the grafting efficiencies), the rubber particles of experiment 2 were smaller than those of experiment 1 (see micrographs of Figs. 4 and 5).

Finally, note that the vitreous occlusions grew along the reaction [cf. Figs. 4(c) and 5(b) with Figs. 4(a) and 5(a)].

Polymerizations with rubber and pure AIBN (experiments 3 and 4)

AIBN radicals actively initiated the monomer but were almost incapable of attacking the rubber. This was confirmed by the very low grafting efficiencies of experiments 3 and 4, which in turn, determined the viscosity plots of experiments 3 and 4 [Figs. 3(a) and 3(b)]. In experiment 3, a rather long phase inversion was observed (from 8 to 20% conversion). The plot of experiment 4 was discontinuous because the viscosity could not be measured in the conversion range 9–21%. The reason for this was that (before the measurements) the reaction mixture demixed into two liquid layers, an upper PB-rich phase and a lower PS-rich phase.

The rate of polymerization of experiment 3 [Fig. 1(a)] was lower than that of experiment C (the equivalent low-temperature prepolymerization without rubber). This reduction could be explained by the relatively high stability of primary rubber radicals and/or an increased cage effect of AIBN radicals in the presence of rubber. In contrast, the conversion plot of experiment 4 [Fig. 2(a)] was practically overlapped with that of experiment D (the equivalent high-temperature reaction without rubber). This was possibly due to a reduction with temperature of the aforementioned effects.

As expected, AIBN lowered the PS molecular weights of experiments 3 and 4 with respect to the initiator-free experiments 1 and 2. This effect was more noticeable in the high-temperature prepolymerization because the initiator was almost totally consumed in this stage.

The morphologies of experiments 3 and 4 are shown in Figures 6 and 7, respectively. In accordance with the viscosity measurements, Figure 6(c) confirmed a phase inversion. In contrast, the characteristic salami particles were not formed in Figure 7(c), suggesting a simple mixture of incompatible liquids.

The final morphology of experiment 3 [Figs. 6(a,b)] consisted of huge particles with large occlusions and a broad PSD. This morphology (i.e., large PS domains mixed with large PB–PS regions) resulted from the combined effects of a low grafting efficiency and low PS molecular weights (which tended to accumulate in the occlusions).

In experiment 4, Figure 7(a,b) confirmed that the phase inversion never took place. This type of morphology was also observed in nonagitated reactions.[16] The PSD of Figure 7(b) was meaningless because independent rubber particles were not formed.

Polymerizations with rubber and pure TBPO (experiments 5 and 6)

Consider the experiments with pure TBPO (a good grafting agent). Compare the low-temperature exper-

iments 5 and E. The reaction rate remained almost unaffected by the rubber [in Fig. 1(a), curves 5 and E are practically overlapped]. In contrast, for the high-temperature experiments 6 and F, the reaction rate was faster with the rubber [Fig. 2(a)]. Two combined effects could explain this last (rather surprising) result. First, the large accumulation of graft copolymer in the PB-rich phase determined an increased gel effect in that phase. Second, there was a preferential accumulation of TBPO into the PB-rich phase, higher than that expected from the thermodynamic equilibrium.[29] To understand this, note that the initiator was added at the start of the prepolymerization when the system still consisted of a single homogeneous rubber-rich phase. Then, after the PS-rich phase was dispersed, the initiator had to slowly diffuse from the original rubber-rich phase into the new dispersed phase. The preferential partitioning of TBPO into the rubber phase also explained the rather large grafting efficiencies of experiments 5 and 6.

Consider the PS molecular weights. As expected, the following was observed: (1) the molecular weights of experiment 6 were lower than those of experiments 5 and 2, (2) the molecular weights of experiment 5 were lower than those of experiment E, and (3) the molecular weights of experiments 3 and 4 (involving pure AIBN) were lower than those of experiments 5 and 6, respectively.

Experiments 5 and 6 exhibited large grafting efficiencies at early conversions. For this reason, neat and fast phase inversions were observed between 10 and 15% conversion [Fig. 3(a,b)]. A high amount of graft copolymer also yielded small final particles (see Table I and Figs. 8 and 9). Furthermore, in experiment 6, a core–shell type of morphology was observed (Fig. 9). The production of core–shell morphologies by rapid transformation of PB into a highly grafted copolymer was previously reported by Moore.[30]

Polymerizations with rubber and initiator mixtures (experiments G and H and 7–12)

For the initiator mixtures, an intermediate behavior between the equivalent 100% AIBN and 100% TBPO cases was generally (but not always) observed.

Consider first experiments 7 and 8, which involved a 50:50 initiator mixture and a stirring rate of 125 rpm. Compare the low-temperature experiment 7 with experiments 3 and 5 and the high-temperature experiment 8 with experiments 4 and 6. As expected, the viscosity plot of curve 7 was intermediate between curves 3 and 5 [Fig. 3(a)]. Similarly, the viscosity plot of curve 8 was intermediate between curves 4 and 6 [Fig. 3(b)]. Like in experiment 5 with 100% AIBN, a demixing of the reaction mixture was observed in experiment 8 between 10 and 21% conversion [see the discontinuity of curve 8 in Fig. 3(b)]. However, this same curve also suggested a curiously late phase inversion in the conversion range 25–35%.

The morphologies of experiments 7 and 8 are presented in Figures 10 and 11, respectively. Figure 10(c) confirmed that (at the prepolymerization end) the system had already inverted phases. In contrast, Figure 11(c) exhibited an unclean phase inversion with ultralarge occlusions. This situation was also reflected in the final morphologies, although Figure 10(a) exhibited a typical salami morphology, Figure 11(a) showed a poor salami morphology. A possible explanation for the large occlusions in experiment 8 was that the low PS molecular weights generated during the (high-temperature) prepolymerization tended to accumulate in the occlusions.

The aim of experiments 7, 9, and 10 was to determine the effect of the stirring rate (125, 250, and 375 rpm, respectively) on the particle morphology. These reactions involved a 50:50 initiator mixture and a prepolymerization at 70°C. The polymerization rates (not shown here for space reasons) were all quite similar. This was also the case for the PS molecular weights (Table I). However, for increasing stirring rates, the grafting efficiencies increased, whereas the particle sizes became smaller. The micrographs of experiments 7, 9, and 10 are given in Figures 10, 12, and 13, respectively. For increasing stirring rates, the final average diameters were reduced from 2.53 μm (experiment 7) to 1.37 μm (experiment 10). In Figures 12 and 13, there was evidence of particle damage by shear stress. Also, an intense micromixing is unfeasible in industrial reactors. For both reasons, the lowest stirring rate of 125 rpm was chosen to carry out most of the prepolymerizations with rubber.

Consider finally experiments 11 and 12 (AIBN/TBPO = 25:75 and 75:25, respectively). The final morphology of experiment 11 is shown in Figure 14. It presented an intermediate situation between a salami and a core–shell morphology. Even though the grafting efficiency could not be measured, it must have been presumably high. This would explain the intermediate morphology of Figure 14, shown at a stage before its dispersion into a core–shell structure. The final morphology of experiment 12 is not presented here, but it was similar to that of the pure AIBN case, with very large particle sizes.

CONCLUSIONS

The bulk HIPS process is highly multivariate, and for this reason, a large number of reactions must be analyzed to understand the complex interrelationships between reaction inputs such as recipe, temperature, and stirring rate and reaction outputs such as conversion, grafting efficiency, molecular structure, and particle morphology.

Most previous publications on the development of the HIPS morphology adopted isothermal prepolymerizations, and BPO has been the most investigated peroxide initiator. In this study, TBPO was the tested initiator, and we considered high-temperature prepolymerizations that included a heating period. Nonisothermal high-temperature prepolymerizations were closer to industrial conditions. However, they were considerably more difficult to analyze because many parameters changed simultaneously during the (crucial) phase-inversion period.

The aim of chemical initiators is to induce rubber grafting early in the prepolymerization. AIBN was unable to attack the rubber. Thus, the grafting efficiencies and morphologies observed with pure AIBN were worse than those of the purely thermal reactions (cf. Figs. 4 and 5 with Figs. 6 and 7). In contrast, when pure TBPO was combined with a high-temperature prepolymerization (experiment 6), a submicrometer core–shell morphology was produced (Fig. 9). This morphology, together with the fast prepolymerization rate of experiment 6 [Fig. 2(a)], made this procedure an interesting and cheap alternative for the production of translucent HIPS films.

The final particle size strongly depended on the shape and size of the rubber particles at the end of prepolymerization. There were three ways to reduce the particle diameters during the phase inversion: (1) an increase in the stirring rate, (2) an increase in the grafting efficiency, and (3) a reduction in the system viscosity. The system viscosity decreased with increasing temperature. An increase in temperature not only affected chain flexibility; it also enhanced the chain-transfer reactions to the monomer, which in turn, lowered the PS molecular weights. However, a reduction in the PS molecular weights during the prepolymerization increased the total volume of the particle occlusions, thus partly compensating for the former effect. This explained why the particle sizes of prepolymerizations at 70°C were not significantly larger than those of equivalent prepolymerizations at 120°C. Adequate control of temperature, initiator type, and stirring rate allowed the production of a large variety of particle sizes and morphologies, which ranged from typical salami structures of average diameters between 1 and 3 μm to submicrometer core–shell particles.

In a future communication, some of the presented results will be used to validate a novel polymerization model that takes into account the heterogeneous nature of the HIPS process.

The authors thank J. L. Castañeda and M. Brandolini for the SEC analyses, N. Casís for her help with the micrographs, and D. Estenoz for the helpful discussions.

References

1. Sudduth, R. J Appl Polym Sci 1978, 22, 2427.
2. Baer, M. J Appl Polym Sci 1976, 20, 1109.
3. Gupta, V. K.; Bhargava, G. S.; Bhattachrayya, K. K. Macromol Sci Chem 1981, 16, 1107.
4. Huang, N. J.; Sundberg, D. C. J Polym Sci Part A: Polym Chem 1995, 33, 2571.
5. Brydon, A.; Burnett, G. M.; Cameron, G. G. J Polym Sci Polym Chem Ed 1974, 12, 1011.
6. Estenoz, D. A.; Valdéz, E.; Oliva, H. M.; Meira, G. R. J Appl Polym Sci 1996, 59, 861.
7. Huang, N. J.; Sundberg, D. C. J Polym Sci Part A: Polym Chem 1995, 33, 2533.
8. Minoura, Y.; Mori, Y.; Inoto, N. Makromol Chem 1957, 24, 205.
9. Minoura, Y.; Mori, Y.; Inoto, N. Makromol Chem 1958, 25, 1.
10. Ghosh, P.; Sengupta, P. K. J Appl Polym Sci 1967, 11, 1603.
11. Brydon, A.; Burnett, G. M.; Cameron, G. G. J Polym Sci Polym Chem Ed 1973, 11, 3255.
12. Huang, N. J.; Sundberg, D. C. J Polym Sci Part A: Polym Chem 1995, 33, 2551.
13. Huang, N. J.; Sundberg, D. C. J Polym Sci Part A: Polym Chem 1995, 33, 2587.
14. Ludwico, W.; Rosen, S. J Polym Sci Polym Chem Ed 1976, 14, 2121.
15. Kehahiov, D.; Mikhnev, B. Int Polym Sci Technol 1985, 12, T/70.
16. Riess, G.; Gaillard, P. Macromol Symp 1983, 221.
17. Estenoz, D. A.; Leal, G. P.; Y. R. López, Oliva, H. M.; Meira, G. R. J Appl Polym Sci 1996, 62, 917.
18. Fischer, M.; Hellmann, G. P. Macromolecules 1996, 29, 2498.
19. Peng, F. J Appl Polym Sci 1986, 31, 1827.
20. Demirrors, M.; Veraert, R.; Hermans, C. Polym Prepr 1999, 40, 71.
21. Polymer Handbook, 3rd ed.; Brandrup, J.; Immergut, E. H., Eds.; Wiley: New York, 1989.
22. Choi, K. Y.; Lei, G. AIChE J 1987, 33, 2067.
23. Kim, K. J.; Ling, W.; Choi, K. Y. Ind Eng Chem Res 1989, 28, 131.
24. Villalobos, M. A.; Hamielec, A. E.; Wood, P. E. J Appl Polym Sci 1991, 42, 629.
25. Solov'eva, I. V.; Bulatova, V. M.; Egorova, E. I.; Kirillova, E. I.; Kusnetzova, S. V. Int Polym Sci Technol 1983, 10, T/45.
26. Kumar, A. Ph.D. Thesis, Carnegie-Mellon University, 1972.
27. Friis, N.; Hamielec, A. E. ACS Symp Ser 1976, 24, 82.
28. Estenoz, D. A.; Meira, G. R.; Gómez, N.; Oliva, H. M. AIChE J 1998, 44, 427.
29. García, N.; Meira, G.; Oliva, H. In Proceedings of the VIII Latin-American Polymer Symposium, Acapulco, México, 10–15 Nov 2002; Polymeric Society of Mexico, 2002, p 321.
30. Moore, J. Polymer 1971, 12, 478.